

RSC Advances



This is an *Accepted Manuscript*, which has been through the Royal Society of Chemistry peer review process and has been accepted for publication.

Accepted Manuscripts are published online shortly after acceptance, before technical editing, formatting and proof reading. Using this free service, authors can make their results available to the community, in citable form, before we publish the edited article. This *Accepted Manuscript* will be replaced by the edited, formatted and paginated article as soon as this is available.

You can find more information about *Accepted Manuscripts* in the [Information for Authors](#).

Please note that technical editing may introduce minor changes to the text and/or graphics, which may alter content. The journal's standard [Terms & Conditions](#) and the [Ethical guidelines](#) still apply. In no event shall the Royal Society of Chemistry be held responsible for any errors or omissions in this *Accepted Manuscript* or any consequences arising from the use of any information it contains.

Pulse electrodeposition and corrosion behavior of Ni-W/MWCNTs nanocomposite coatings

Han Li^c, Yi He^{a,b,c*}, Yi Fan^c, Wei Xu^c, Qiangbin Yang^c

- a. State Key Lab of Oil and Gas Reservoir Geology and Exploitation (Southwest Petroleum University), Rd.8, Xindu District, Chengdu City, Sichuan Province, P.R. China, 610500*
- b. Oil & Gas Field Applied Chemistry Key Laboratory of Sichuan Province, Southwest Petroleum University, Chengdu City, Sichuan Province, P.R. China, 610500*
- c. College of chemistry and chemical engineering, Southwest Petroleum University, Chengdu City, Sichuan Province, P.R. China, 610500*

**Address correspondence to this author. E-mail: heyi007@163.com, Phone and Fax: +86*

02883037315

Abstract

In this study, Ni-W/multiwalled carbon nanotubes (MWCNTs) composite coatings were successfully deposited on the surface of C45 steel sheet by pulse current electrodeposition. Particularly, a uniform dispersion of MWCNTs in the plating electrolyte bath is indispensable. To achieve this main point, MWCNTs were modified by acidification, and coupled with introduction of sodium dodecyl sulfate to the plating bath. Scanning electron microscopy (SEM) and X-ray diffraction (XRD) were employed to characterize the morphology and structure of the composite coatings. The corrosion behavior of the composite coatings on steel was investigated by polarization curves and electrochemical impedance spectroscopy (EIS) in 3.5 wt-% NaCl aqueous solutions with pH of 10, 7, 3 and 10 wt-% HCl solutions at various temperatures, which are representative of corrosive environments of relevance to many engineering applications. The result indicates that the incorporation of MWCNTs made Ni-W composite coatings compact and uniform. Consequently, a higher corrosion resistance and thermal stability of Ni-W/MWCNTs deposits were obtained. The optimal concentration of MWCNTs in the bath is 2 g L^{-1} .

Keywords: Ni-W composite coatings, multiwalled carbon nanotubes, corrosion resistance, pulse electrodeposition

1 Introduction

Electrodeposited coatings containing reinforcement particles have been considered for many applications largely because of their excellent mechanical, electrochemical and oxidation properties. Among the matrix of composite film made up of alloy or metal, electrodeposited Ni-W coating is used as a functional coating that exhibits superior mechanical and chemical properties. Recently, Ni-W alloy coatings have been developed as a kind of surface treatment for substituting the environmentally harmful hexavalent hard chromium film for their unique characteristics, such as high hardness, good wear resistance and corrosion resistance [1-3]. Moreover, prior studies have shown that Ni-W coatings exhibited a clearly increased corrosion resistance compared to pure Ni coating. For example, Alimadadi et al.[4] recorded that in 3.5 wt-% NaCl aqueous solution, the polarization resistance of Ni-W alloy coatings generally decreased with increase of W content (0-25.7 at.-%) and with reduction in crack density. Yang et al. [5] reported that application of heat treatment at 400°C for 1 h increased the corrosion current density (i_{corr}) and the corrosion potential (E_{corr}) of Ni-W alloys in 3.5 wt-% NaCl solution, due to grain boundary relaxation upon heat treatment. In a more engineering-oriented work, Jones et al. [6] reported that Ni-W coatings could effectively shield steel substrates from corrosion in standard neutral salt spray testing. However, the undesired residual stress frequently increases with increasing hardness and wear resistance, so dispersoids are widely used in composites to provide low residual tensile stress. Recently, in the field of galvanic deposition, various Ni-W-based composite films containing micro- and

nano-sized inorganic inert particles that have been developed through the electrodeposition technique involving Ni-W-Al₂O₃ [7-8], Ni-W-TiO₂ [9], Ni-W-diamond [10], Ni-W-SiC [11], Ni-W-WC [12], Ni-W-CeO₂ [13], Ni-W-Co [14], Ni-W-B [15], and Ni-carbon nanotubes (CNTs) alloys [16-18]. Moreover, the studies suggested that reinforcing particles conferred to these coatings improved corrosion and wear resistance, hardness, and adhesion of future paint layers and increased the life-time of the coatings [19]. The characteristics of composite coatings strongly rely on the nature of the particles and their contents. It is well known that pulse current composite electrodeposition [20] is one of the most effective techniques for producing nanocomposites of metallic and nonmetallic constituents with low cost. And pulse electrodeposition is a valuable way of co-depositing fine phase with the ability of improving the surface quality and the mechanical properties of the coatings. In addition, pulse plating offers a greater control over the structure and properties of electrodeposits compared to the conventional direct electrodeposition. This technique yields more uniform and homogeneous deposits with fine grains and limits amount of defects [21]. Pulse current electrodeposited coatings have better tribological and mechanical properties compared to direct current electrodeposits [22-23]. Hence, pulse current plating has replaced direct current plating as a significant method for the deposition of composites.

In recently years, theoretical and experimental researches have demonstrated that multiwalled carbon nanotubes (MWCNTs) show a promising potential as a reinforcing phase to endow organic and inorganic composite coatings with excellent

wear resistance and minimal coefficient of friction [24-25], owing to their particular properties, such as multilayer stripe structure, high electrical conductivity [26], lubricity, chemical stability, and extremely high strength [27]. MWCNTs have been revealed as effective filler for reinforcing Ni electrodeposits to improve hardness, wear resistance and corrosion resistance [28-30]. Khabazian and Sanjabi [28] confirmed that the hardness and the corrosion resistance of the deposited Ni coating were greatly improved by the incorporation of modified MWCNTs. Martis et al. [29] reported the mechanical properties of Ni coating were improved by incorporating different kinds of surface functionalized MWCNTs. Carpenter et al. [30] found that the surface-modified CNTs significantly improved the wear resistance of the reinforced Ni coatings. Though the bulk of the literatures concerning MWCNTs reinforced Ni or Ni-based alloy system were reported, only a few researchers have concerned the synthesis and properties of MWCNTs reinforced Ni-W alloy coatings. Moreover, MWCNTs in the original state are easily prone to agglomeration in polar solvents (such as an electrolyte bath) due to its high van der Waals interaction energy and aspect ratio [31]. The agglomeration of MWCNTs in the electrolyte reduces the deposition efficiency of MWCNTs and may have adverse effects on the physical properties of the electrodeposits. One of the chief problems is the acquisition of a uniform distribution of MWCNTs in the plating electrolyte bath. In current research, MWCNTs are pretreated by a series of functionalizing treatments (such as acid refluxing treatment) [32] that can improve dispersal stability in polar solvents. Furthermore, surfactants are applied in plating bath for the stability of nanoparticles.

The focus of this work is on the investigation of Ni-W/MWCNTs composite coatings with different contents of MWCNTs deposited on the surface of C45 steel sheet by pulse current electrodeposition. The morphology and microstructure of Ni-W/MWCNTs composite coatings are characterized by scanning electron microscopy (SEM) and X-ray energy-dispersive spectrometry (EDS). Apart from these, the corrosion resistances of resulting MWCNTs composite coatings in 3.5 wt-% NaCl solutions with pH of 10, 7, 3 and 10 wt-% HCl solutions were also studied in detail.

2 Experimental methods

2.1 Treatment of MWCNTs

MWCNTs with an average diameter of 20-30nm and an average length of 10-30 μ m were obtained from the Institute of Organic Chemistry, Chengdu, China. To improve the dispersibility during electroplating and consequently their homogeneity in the electrodeposits, MWCNTs were first subjected to a functionalizing acid treatment in a mixed solution of 98% concentration sulfuric acid and 70% concentration nitric acid (v:v = 1:2) at 130°C for 2h [27]. It is well known that the oxidation procedure in acidic solution can introduce different hydrophilic oxygen-containing functional groups on the surface of MWCNTs (mainly carboxylic groups) which promotes the dispersion of MWCNTs in the solvent by electrostatic repulsion [33-34]. Next, the MWCNTs were divided from the solutions through three cycles of dilution with deionized water continued by sedimentation. Finally, the modified MWCNTs with a shorter length were collected after the evaporation of the

deionized water.

2.2 Electrodeposition of Ni-W/MWCNTs nanocomposite coatings

Ni-W/MWCNTs composite coatings were co-deposited by pulse current electrodeposition technique with the operational parameters shown in Table 1. In particular, sodium dodecyl sulfate (SDS) was used as a dispersion agent in the plating baths to further maintain the homogeneous dispersion and the stability of MWCNTs while stirring [35]. Furthermore, mechanical agitation was used for dispersion and deagglomeration of nanoparticles into liquids during the plating process. All chemicals were analytical-grade reagents and the deionized water was of ultra-high purity (with a conductivity of $0.055\mu\text{s}/\text{cm}$). For electrodepositing various Ni-W/MWCNTs nanocomposite coatings, the modified MWCNTs concentrations were set to be 0, 1, 2, 3, and 5g L^{-1} , respectively. The pH of the electrolyte was adjusted by adding citric acid. Prior to electrodeposition, the electrolyte was subjected to an intense ultrasonic treatment to fully disperse the suspended MWCNTs. The C45 carbon steel sheet of $15\text{mm}\times 30\text{mm}$ in dimensions formed a working cathode with an approximate active area of around 1cm^2 , while the graphite electrode with an approximate area of 42cm^2 was used as working anode. Before the coating was deposited, the substrate was first polished using 600, 800 and 1200 grit emery-paper, and then ultrasonically cleaned with acetone to remove contaminations, followed by cleansing with deionized water. Afterward, the surface of the substrate was activated by using 1M sulfuric acid solution at room temperature for 30s, washed with distilled water and then quickly dipped into the plating bath. During deposition, the electrolyte

was stirred at a constant speed of 100rpm using a magnetic stirrer. Finally typical Ni-W/MWCNTs composite coatings with a thickness of around 30 μ m were obtained.

The schematic diagram of the electrodeposition setup is shown in Fig. 1.

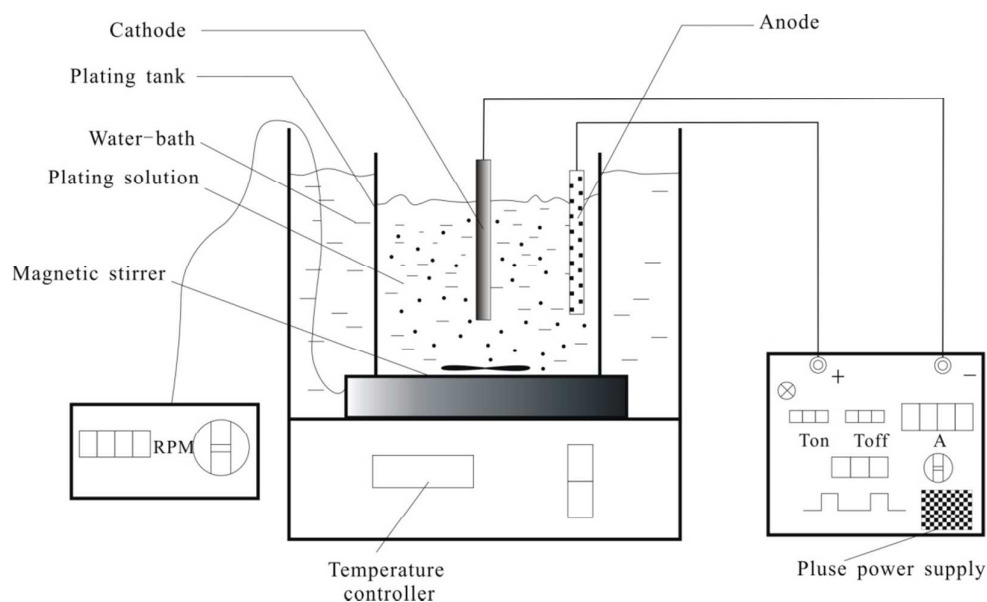


Fig1. The schematic representation of the electrodeposition setup

Table 1 Bath composition and operating conditions for the preparation of Ni-W/MWCNTs composite coatings

Chemicals	Composition (g L ⁻¹)	Plating parameters
NiSO ₄ ·6H ₂ O	15.8	5 A dm ⁻²
Na ₂ WO ₄ ·2H ₂ O	46.2	pH=7.5
NaBr	15.5	t=1h
Na ₃ Cit	147.0	T=65~75 °C
NH ₄ Cl	26.7	f=1000HZ
Sodium dodecyl sulfate	0.1	r(duty cycle)=0.8
MWCNTs	0,1,2,3,5	

2.3 Characterization of coatings

The morphologies of the surface and the element compositions of the coatings were characterized by scanning electron microscopy (SEM; JSM-7500F, JEOL) and X-ray energy-dispersive spectrometry (EDS; INCA), respectively. The distribution of MWCNTs in the composite coatings were analysed using the backscattered

(BS)-SEM method. The grain structure and crystals orientation were studied using X-ray diffraction (XRD; PANalytical X'Pert Pro diffractometer) with Cu K α radiation (1.5405 Å). The scanning angle (2θ) range from 30° to 80°, with a step size of 0.02° and counting time of 2 s/step. The coating thickness was measured by QNix 4500 coating thickness gauge, and then calculated by averaging over five tests for each sample.

2.4 Immersion tests

The immersion tests were carried out to evaluate the corrosion rates (mass losses) of the composite coatings with different MWCNTs concentration. For comparison, pure Ni-W-coated and uncoated carbon steels were also used. The coating thickness prepared for immersion tests were around 30 μm since the coatings were prepared according to the same procedures. The corrosion resistance in solution consisting of 3.5 wt-% NaCl at room temperature was determined by measuring weight change. The reported corrosion rates are steady-state values determined from slope of weight loss vs time (240 h) curves. Before the corrosion tests, the sample was measured and weighed on a scale accurate to 0.01 mg. After the experiment was finished, the sample was cleaned with acetone, followed by drying under vacuum condition, and then weighed again. Afterward, the corresponding mass loss per unit surface area of the coatings was calculated.

2.5 Electrochemical measurement

Electrochemical tests were used to evaluate the corrosion resistances of the electrodeposits. These tests were carried out by using a conventional three-electrode

cell with a platinum plate as the counter electrode and a saturated calomel electrode (SCE) as the reference electrode. Electrodeposited samples with around 1cm^2 exposed areas were used as the working electrode. The test solutions were 3.5 wt-% NaCl aqueous solutions with different pH's (10, 7, and 3) and 10 wt-% HCl solutions at room temperature. Electrochemical impedance measurements were carried out under the frequency range of 10^{-2} - 10^5 Hz with an AC amplitude of 10mV at the open circuit potentials. Potentiodynamic polarization tests were taken by sweeping the potential over the range of 250mV vs. the SCE below open circuit potential (OCP) to 1000mV vs. the SCE at a scanning rate of 1mVs^{-1} . Through the intersection of the anodic and cathodic Tafel curves employing the Tafel extrapolation method, the values of corrosion current density (I_{corr}) and corrosion potentials (E_{corr}) were calculated. The analysis of the spectra was performed using the ZView (version 3.2) software. Before all the measurements, the working electrodes were immersed in the corrosive media for 2 h to stabilize the OCP. The curve for open-circuit potential vs. times was measured in 3.5 wt-% NaCl aqueous solution. The open-circuit potential was recorded with respect to a saturated calomel electrode every 30 min for a period of 15h. The measurements of potentiodynamic polarization were made with regard to the open-circuit potential.

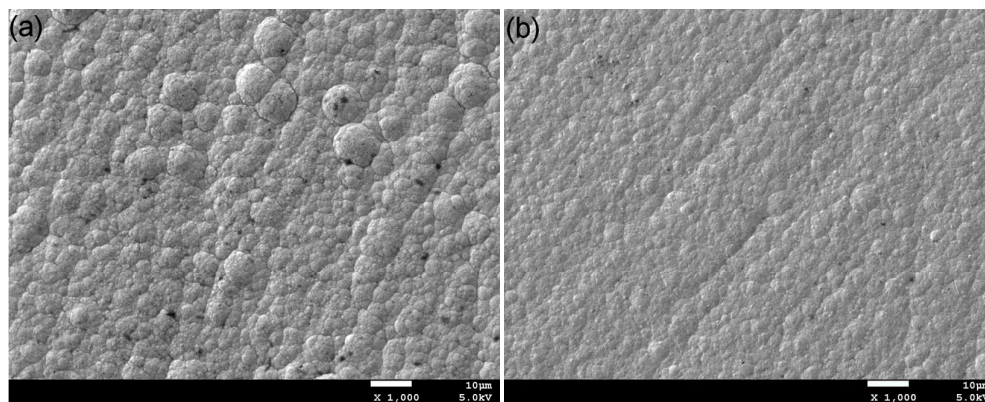
3 Results and discussion

3.1 Morphology and microstructure of composite coatings

The Ni-W/MWCNTs composite coatings were prepared by co-depositing MWCNTs with Ni-W alloy under magnetic agitation. The SEM images of the typical

surface morphology and the corresponding EDS mapping analysis of the composite coatings obtained under various conditions are shown in Figure 2. As seen in figure, the Ni-W/MWCNTs coatings (Figure 2b) form a much more uniform, smooth, and compact surface structure compared to Ni-W coatings (Figure 2a) because of the effect of nanoparticles. Nonetheless, the morphology of Ni-W/MWCNTs coatings also contains bulge parts distributed on the surface of coatings. And the surface roughness and nonuniformity increased with increasing concentration of MWCNTs, due to the MWCNTs cohering and forming secondary particles in composite plating baths when the MWCNTs concentration is larger than 2 g L^{-1} [36]. The EDS mapping analysis demonstrates that the MWCNTs are uniformly distributed in the Ni-W alloy matrix. Figure 2e-f reveals the C elemental contents tested by EDS of the composite coatings that are fabricated with various concentrations of MWCNTs (1, and 2 g L^{-1}). On the basis of the experiments, the MWCNTs content of the coating matrix increased with increasing MWCNTs concentration in the plating bath. Since in this system, there was a competition between MWCNTs and metals during the co-deposition process, and the MWCNTs can be absorbed onto the surface of the cathode to provide a great deal of nucleation sites for the metals [37]. These nanoparticles would shield the growth of crystals. Thus, this effect decelerated the Ni and W deposition rate, yielding smaller and better grain sizes of metals that co-deposit with more MWCNTs, finally forming a compact and uniform coating structure. This phenomenon can be explained by Gugliemi's two-step adsorption model [38]. While the particles are adsorbed, metal begins forming slowly around the cathode, encapsulating and

incorporating the particles. However, it is noticeable that MWCNTs are easy to agglomerate in aqueous solution, and a high concentration of MWCNTs will lead to enhancement of agglomeration in both the matrix and the plating bath, which results in the difficulty of adsorption of particles and influences the structure of composite coatings. Therefore, there should be an optimum concentration of MWCNTs for preparing the Ni-W/MWCNTs composite coating by electrodeposition as the preparation of composite coating embedding CNTs by electroless plating [39], at which a high output of Ni-coated MWCNTs with good morphology can be obtained. A cross-sectional SEM image of Ni-W/MWCNTs coating containing 2 g L^{-1} MWCNTs is shown in Figure 2g. Obviously, the coating was smooth and compact and, at the same time, had a good adhesion with the matrix steel. Figure 2h shows a backscattered SEM (BS-SEM) image of the surface of cross-section of the Ni-W/MWCNTs composite coating containing 2 g L^{-1} MWCNTs. In the BS-SEM image, the lower atomic mass of carbon nanotube appears black against the gray Ni-W matrix. It is noticeable that the uniform dispersion of MWCNTs in the deposits is acquired.



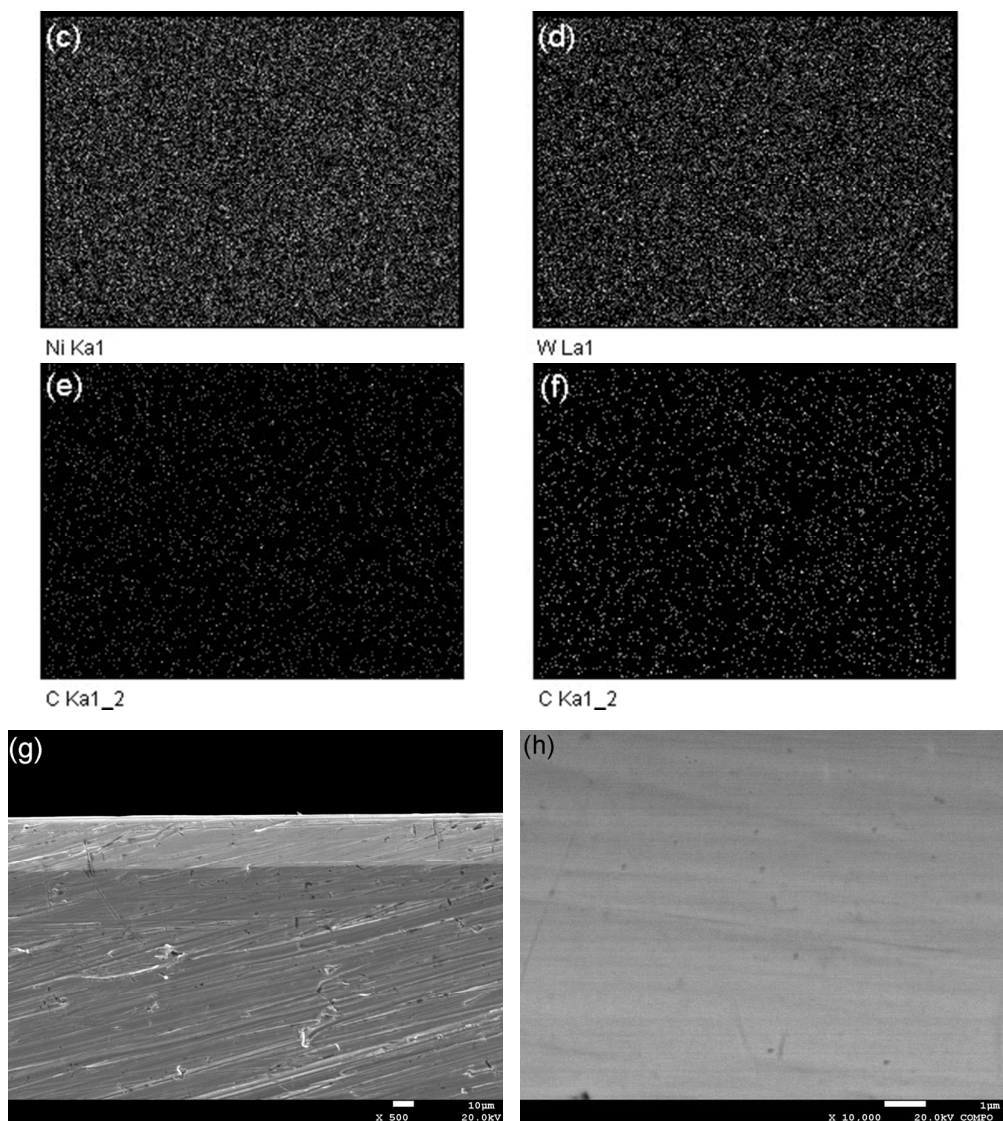


Fig.2 SEM images of Ni-W/MWCNTs coatings surface containing (a) 0 g L^{-1} , (b) 2 g L^{-1} of MWCNTs and corresponding Ni(c), W(d), C mapping of the composite coatings on C45 steel with (e) 1 g L^{-1} , (f) 2 g L^{-1} MWCNTs contents, and Cross-sectional SEM image (g) and its backscattered SEM image (h) of Ni-W/MWCNTs coatings containing 2 g L^{-1} of MWCNTs

Figure 3 reveals the incorporation of MWCNTs into the growing Ni-W matrix schematically. During the early stage of electrodeposition (Figure 3a), MWCNTs are mechanically entrapped into the growing Ni-W matrix. Due to non-metallic MWCNTs, inclusion of them into the Ni-W matrix reduces the surface of cathode and

by prolonging time of deposition (Figure 3b), the nickel ions and tungsten ions are reduced uniformly on the cathode surface apart from the areas where MWCNTs are presented. This process is continuous until MWCNTs are buried into the growing matrix to form final composite coating with a smooth surface (Figure 3c).

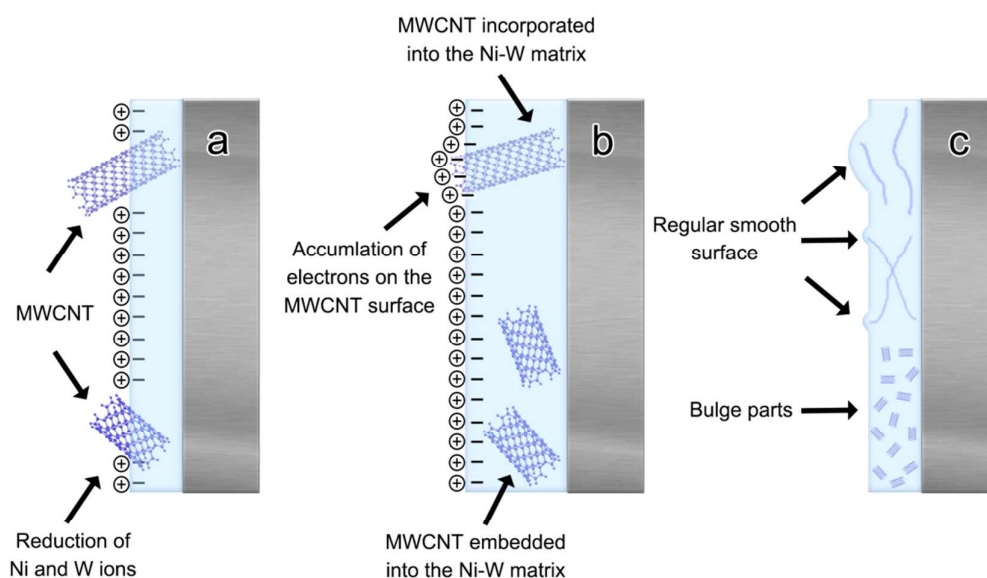


Fig.3 (a) initial stage of the electrodeposition, entrapment of MWCNTs into the growing matrix, (b) creation of bulge parts on the incorporated MWCNTs and embodiment of MWCNTs into the matrix, (c) formation of final composite coatings

Figure 4 shows the XRD patterns of the Ni-W/MWCNTs composites and Ni-W alloy coating. The patterns reveal the crystalline fcc structure of the coatings with predominant plane (1 1 1). The absorption intensity of the diffraction peak decreased with the addition of MWCNTs. This implies that the effect of grain refinement of the nanoparticles in the metal matrix improves the structure of the composite coating and makes it compact, homogeneous, and better grained [40]. The crystallite sizes were calculated for both the Ni-W/MWCNTs and Ni-W composite coatings using

Scherrer's equation (1), where D is the crystallite size (nanometers), K is the shape factor (typical value is 0.89), λ is the incident radiation (1.5418 Å), B is the corrected peak width (radians) at half-maximum intensity, and Θ is Bragg's angle (degrees):

$$D = \frac{K\lambda}{B \cos \vartheta} \quad (1)$$

The sizes of the (1 1 1) planes of the electrodeposited coatings and the corresponding coating thickness are listed in Table 2. The Ni-W/MWCNTs composite coating with MWCNTs concentration in the plating bath of 2 g L⁻¹ (C2) has the smallest crystals. It shows that the addition of MWCNTs decreased the crystallite sizes of the coating and slightly increased the coating thickness. Briefly, suspended MWCNTs adsorbed ions and complexes showed in the electrolyte such as [(Ni)(HWO₄)(Cit)]²⁻ [41]. When the Ni-W matrix growing centers are doped with MWCNTs, the adsorbed complexes and ions shield the growing centers from cations in the electrolyte and inhibit the further growth of Ni-W grains. In general, during the process of plating, the inclusion of suspended particles in the matrix growing centers can decrease the grain size of the metal matrix by means of offering nucleation sites for reducing metallic ad-atoms and inhibiting grain growth.

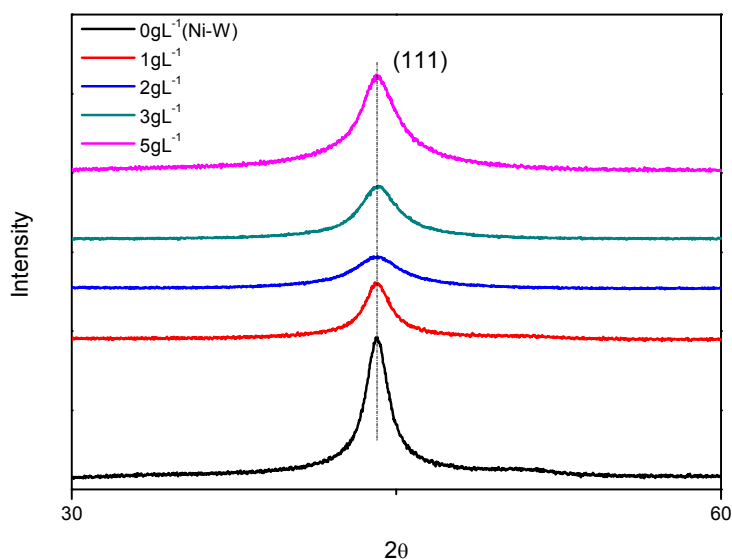


Fig.4 XRD Patterns for Ni-W/MWCNTs composite coatings with different concentration of MWCNTs

Table 2 Crystallite size of the composite coatings containing various concentrations of MWCNTs

Deposits(g L^{-1})	0	1	2	3	5
Crystallite size /nm	23	12	9	15	18
Thickness/ μm	27	29	31	30	28

3.2 Corrosion rate

After immersion tests in 3.5 wt.% NaCl solution for over 240 h, the surface of the Ni-W/MWCNTs coating retained original gloss, although weight loss had occurred, while the surfaces of the Ni-W coated and uncoated carbon steels became uneven, rough and lost brightness. Figure 5 shows the weight loss data resulting from immersion test for 240 h in 3.5 wt.% NaCl solution for five samples. It can be observed that the Ni-W coated sample exhibited higher corrosion rate than that of Ni-W/MWCNTs composite coating. It is obvious that the presence of MWCNTs in the deposit significantly decreased the corrosion rate of the coating, and the composite coating with MWCNTs concentration is 2 g L^{-1} showed the best corrosion resistance.

The inclusion of MWCNTs provided better anti-corrosion property to the Ni-W/MWCNTs composite coatings [42]. The corrosion resistance of the Ni-W/MWCNTs coating was seven times and four times of those of the bare and Ni-W coated samples, respectively.

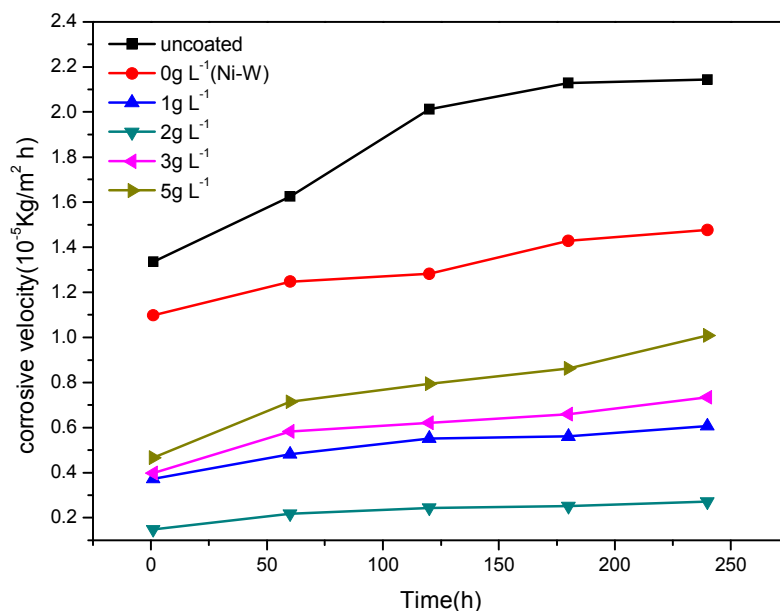


Fig.5 Variation of the corrosion rate (mass losses) with immersion time for uncoated, Ni-W coated and Ni-W/MWCNTs coated samples in 3.5wt-% NaCl solution

3.3 Electrochemical characterization

The corrosion resistance of the composite electroplated coatings was measured by electrochemical impedance spectrum and potentiodynamic polarization curves in 3.5 wt-% NaCl solution. The EIS spectra revealed the impedance message for the deposits exposed in corrosive solutions for 1 h. Figure 6 shows open-circuit potential (E_{ocp}) vs. time curves for various coatings. It is observed that the potentials were strongly modified during immersion. With immersion time increasing, E_{ocp} for Ni-W coating not only was lower than that for the Ni-W/MWCNTs coated sample, but also evolved slowly. For the Ni-W/MWCNTs coatings, a stationary value was obtained

after about 2h of the immersion, exhibiting excellent chemical stability. These results show that the addition of MWCNTs in the Ni-W coating significantly increased E_{ocp} towards more positive values, reducing the tendency towards galvanic corrosion.

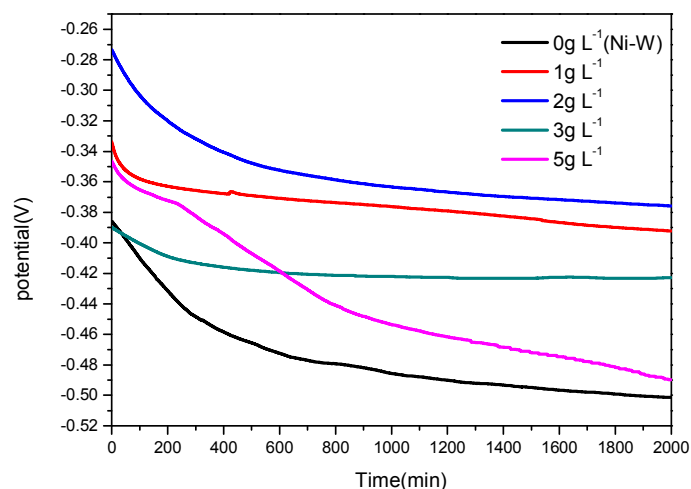


Fig. 6 Variation of the open-circuit potential with the immersion time in 3.5% NaCl solution for the samples

Figure 7 presents the Nyquist plots for the Ni-W alloy and Ni-W/MWCNTs coatings prepared with different contents of MWCNTs. It can be seen that the addition of MWNTs does not significantly change the shapes of EIS, thus not altering the reaction mechanism of Ni-W reduction. The real impedance of the Ni-W coating is much smaller than that of the Ni-W/MWCNTs coating, which is accordance with immersion test results stating that the incorporation of the MWCNTs has greatly improved the corrosion resistance of the Ni-W/MWCNTs composite coatings. And the radius of impedance of composite coatings is significantly increased with MWCNTs incorporation. The specimen obtained with 2g L⁻¹ MWCNTs has the largest radius of impedance semicircle. The observed Nyquist plots for all the deposits implied a simple RQ circuit and the fitted plots are also shown in Figure 6. To explain

the corrosion behavior of the coatings, an equivalent electrical circuit model, as shown in Figure 8, was utilized to simulate the metal/solution interface and to analyze the Nyquist plots. In this figure, R_s is the solution resistance and R_{ct} is charge transfer resistance, which is proportional to the corrosion resistance. Constant phase element (CPE) was used to substitute ideal capacitors [47] to which is attached a phenomenological constant n often used to fit impedance behavior at electrode/electrolyte interface which shows deviation from real capacitor behavior. According to the literature [43], CPE_{dl} values can be related to the surface inhomogeneity and porosity of the coating. Table 3 shows that the charge transfer resistance (R_{ct}) increased with the incorporation of MWCNTs into the composite coating, thereby increasing the corrosion resistance of the coating, while the CPE of electric double layer capacitance (CPE_{dl}) values decreased with incorporation of MWCNTs. These results are attributed to the role of the MWCNTs in modifying the structure. The nanoscale deposited MWCNTs reduce the structural and surface defects by filling the crevices, gaps, and micron holes of the coating [44-45]. Usually, noble metal films provide a barrier to protect steel against corrosion or other damages. However, the current research found that Ni dissolved easily from the alloy matrix because of galvanic action [9], while Ni-W/MWCNTs coatings were found to be compact and smooth. Consequently, it is clear that MWCNTs incorporation blocked the dissolution of Ni and the diffusion of corrosive media through adsorbing on the anodic sites, leading to the formation of a more homogenous and dense coating.

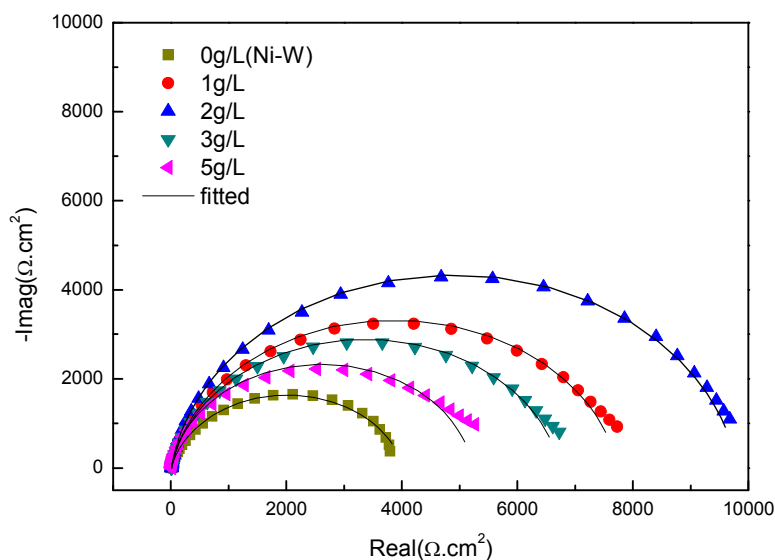


Fig.7 Electrochemical impedance Nyquist plots of the composite coatings

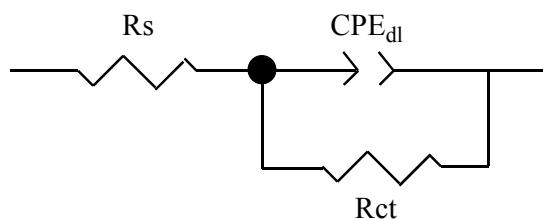


Fig.8 Equivalent electrical circuit model used to analyze the EIS data

Table 3 Values of the workers resulting from the fitting of equivalent circuit with experimental plots

Deposits (g L ⁻¹)	R _s (Ω.cm ²)	R _{ct} (Ω.cm ²)	Q _{dl} (F)	n
0	8.6	4019	5.35×10 ⁻⁵	0.8
1	10.3	7728	3.93×10 ⁻⁵	0.8
2	13.9	9784	3.49×10 ⁻⁵	0.8
3	12.7	6439	4.32×10 ⁻⁵	0.8
5	11.3	5209	5.13×10 ⁻⁵	0.8

The measured potentiodynamic polarization plots of the Ni-W and the different Ni-W/MWCNTs composite coatings in the as-deposited condition in 3.5 wt-% NaCl solution are illustrated in Figure 9. All the Tafel curves of Ni-W and Ni-W/MWCNTs coatings are slightly analogous to each other in terms of shape. The values of corrosion potential (E_{corr}) and corrosion current densities (i_{corr}) were obtained through

extrapolating the linear segments of the cathodic and anodic curves to the intersection, and summarized in Table 4. The slopes of these linear segments were used to calculate Tafel slopes. According to the theory of electrochemistry, i_{corr} is inversely proportional to charge transfer resistance (R_{ct}). That is, MWCNTs increased R_{ct} indicates decrease in i_{corr} values [46]. Ni-W/MWCNTs deposits exhibit higher corrosion potential and lower corrosion current density compared to Ni-W coatings. This means that the corrosion resistance increased with the incorporation of MWCNTs to the Ni-W matrix. Particularly, when the concentration of MWCNTs in plating bath was 2 g L^{-1} , not only the corrosion potential increased significantly, but also the anodic corrosion current density decreased rapidly. Additionally, the incorporation of the MWCNTs decreased the cathodic Tafel slope but increased the anodic one. Furthermore, with anodic polarization potential increasing to a positive value, the corrosion current began to increase slowly, showing a passive behavior. In view of this, it is evident that MWCNTs play an important role in the passivation process of the composite coating [47]. Owing to the great difference in self-potential between the Ni-W matrix and MWCNTs, the passivation process occurred on the surface of the Ni-W coating blocked the supply of water to the electrode surface, therefore preventing the hydration of Ni-W substrate. The improvement of the corrosion resistance of the Ni-W/MWCNTs composite coating can be related to the acceleration of the chemical passivation to some extent. In Figure 10, the SEM images of the surface morphology of the samples taken after the polarization measurements can verify the consequence. It is obvious that the corresponding surface of the Ni-W deposit involved some holes,

pits, and cracks, while the corroded surface of Ni-W/MWCNTs coatings were smooth, compact, and uniform. Two main reasons can account for the good electrochemical performance of composite coatings. Firstly, the gaps, crevices, and micro holes of the Ni-W matrix could be filled by co-deposited MWCNTs, which played the role of physical barriers to the growth of defect corrosion [48]. Secondly, the homogeneous distribution of MWCNTs enhances the corrosion potential of coatings as well as decreases the corrosion current. As a result, uniform corrosion has priority to take place while localized corrosion is inhibited[49].

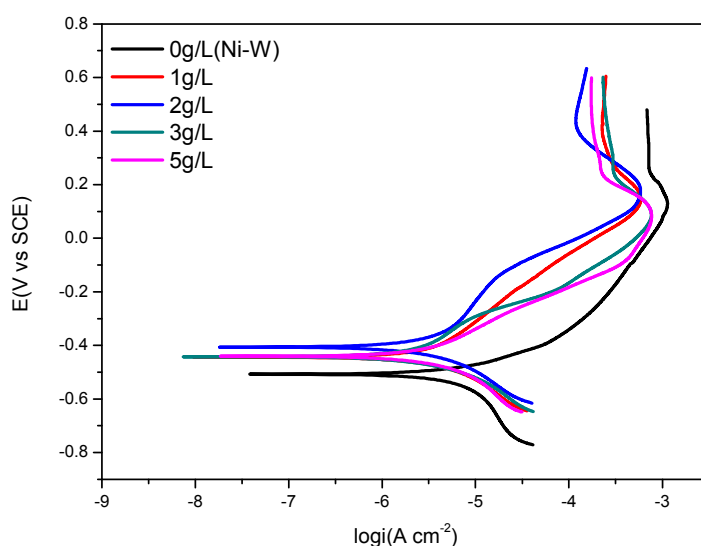


Fig.9 polarization curves of the composite coatings in 3.5 wt-% NaCl solution

Table 4 Corrosion potentials and corrosion current densities of the composite coatings containing various concentrations of MWCNTs

Deposits(g L ⁻¹)	OPC vs SCE (V)	E _{corr} vs SCE (V)	i _{corr} (uA cm ⁻²)
0	-0.51	-0.49	8.03
1	-0.37	-0.36	2.60
2	-0.35	-0.31	1.76
3	-0.41	-0.39	2.98
5	-0.49	-0.43	3.94

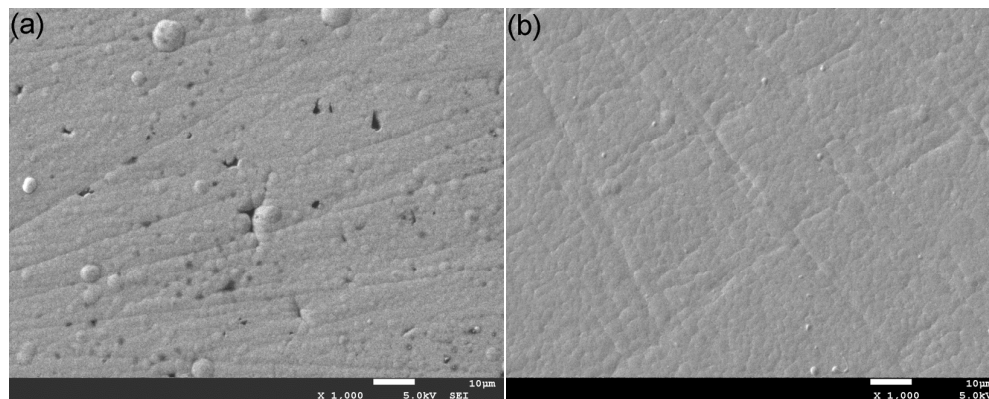


Fig.10 Morphology of samples after potentiodynamic tests in 3.5 wt-% NaCl solution: (a) Ni-W (0 g L^{-1}); (b) Ni-W/MWCNTs (2 g L^{-1})

Next, the performances of the composite coating platings with 2 g L^{-1} MWCNTs were investigated in 3.5 wt-% NaCl electrolyte with pH of 10, 3 and 10 wt-% HCl aqueous solutions. The electrochemical curves of the deposits tested in 3.5 wt-% NaCl solution with pH of 10 are presented in Figure 11a-b. From the Nyquist plots, compared with the Ni-W deposit, the Ni-W/MWCNTs composite coatings have a significant increase in corrosion resistance. As Figure 11b shows, E_{corr} noticeably increases from -0.45 to -0.32V vs. SCE and the passive current density decreases clearly.

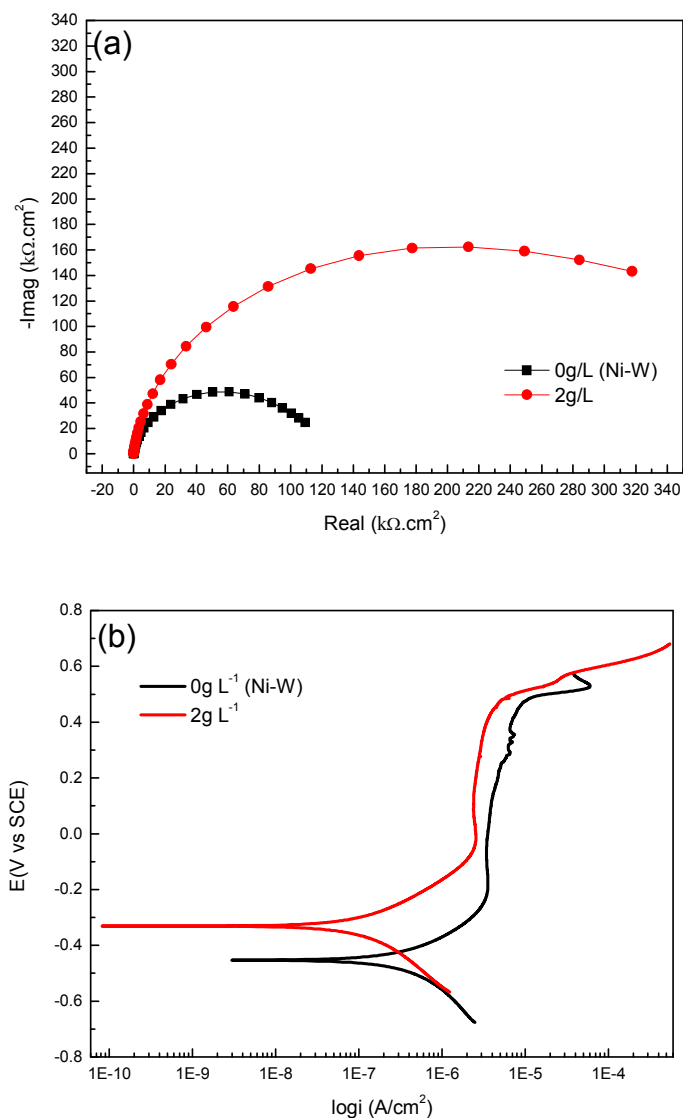
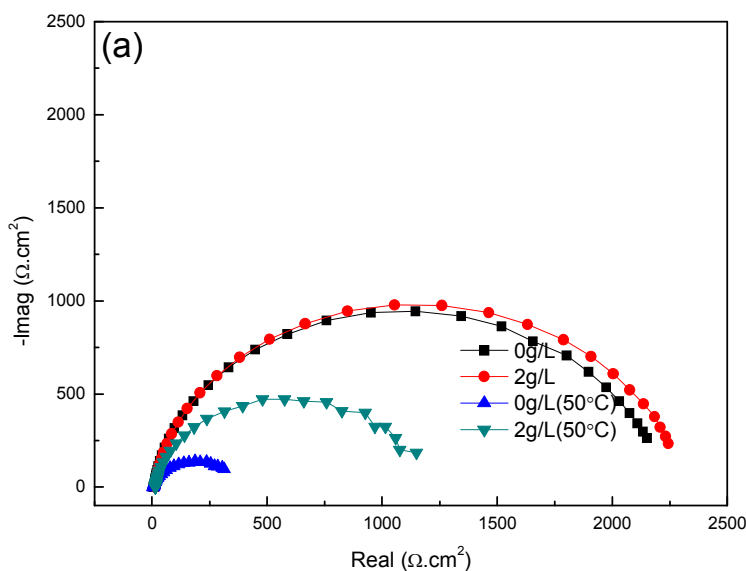


Fig.11 Electrochemical curves of the samples tested in 3.5 wt-% NaCl solution with pH 10: (a) Nyquist plots; (b) polarization curves

Figure 12 presents the Nyquist plots and the polarization curves of the specimens studied in 3.5 wt-% NaCl solution with pH of 3. In the case of room temperature, although the E_{corr} of the composite increased (-0.25 to 0.21), the passive current density increased as well. It should be noted that the Ni-W/MWCNTs composite is not obviously superior at room temperature. While, during the high temperature

process (50°C), the composite coatings exhibit a better stability and corrosion resistance compared to the Ni-W deposit. E_{corr} and i_{corr} noticeably increased and decreased, respectively. The same stability at room temperature could be attributed to the formation of a similar passivation film which can inhibit the dissolution of matrix in acid medium, consequently increased the corrosion resistance of coatings. However, with an increasing temperature, the stability of the passivation film becomes poor, and the dissolution rate of the surface passivation film is greater than the rate of formation. Therefore, a dense and compact structure will hold the corrosion resistance when the passivation film becomes poor.



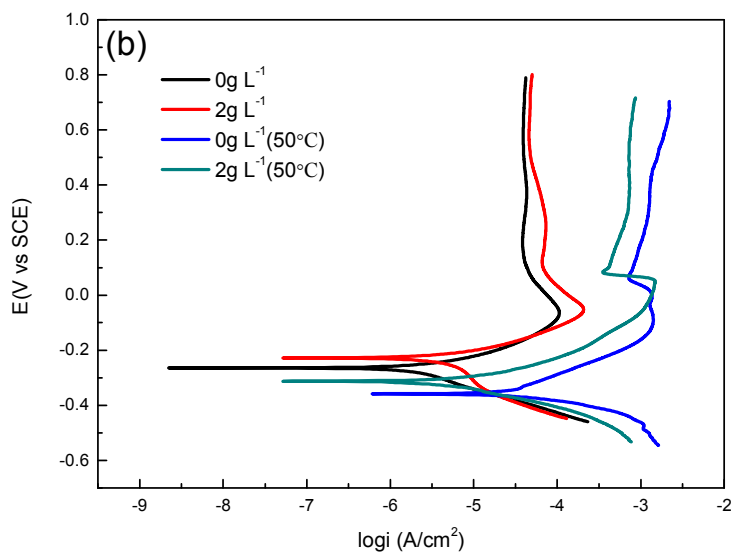


Fig.12 Electrochemical curves of the samples tested in 3.5 wt-% NaCl solution with pH 3: (a) Nyquist plots; (b) polarization curves

An acidic medium is a common corrosion environment, and the behaviors of the deposits were investigated in 10 wt-% HCl solution as well. Figure 13 shows the electrochemical curves of the Ni-W/MWCNTs and Ni-W coatings. Apparently, the incorporation of MWCNTs improves the corrosion resistance of the composite coatings. On the other hand, at room temperature, Ni-W/MWCNTs perform better than Ni-W in the concentrated acid solution. In conclusion, the performance of the Ni-W/MWCNTs composite coatings is improved in both acid and saline solutions, and the composite coatings have better temperature stability.

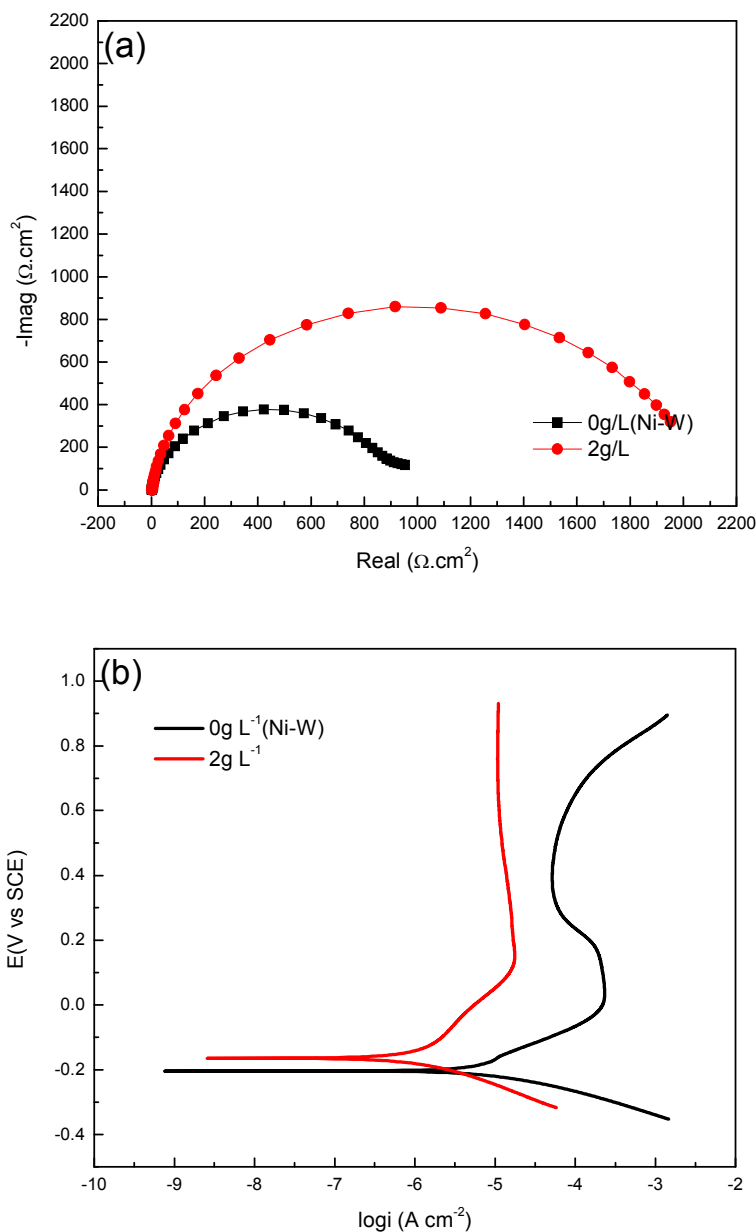


Fig.13 Electrochemical curves of the samples tested in 10 wt-% HCl solution:
(a) Nyquist plots; (b) polarization curves

4 Conclusion

Ni-W/MWCNTs composite coatings were successfully fabricated by pulse current electrodeposition with homogeneous distribution of MWCNTs throughout the Ni-W alloy matrix. The related corrosion studies show that the incorporation of MWCNTs into the alloy matrix significantly increased the corrosion resistance. In

addition, the best performance of composite coatings on steel was that of the specimen which had been treated with 2 g L^{-1} MWCNTs. The improvement in corrosion resistance is attributed to the MWCNTs acting as physical barriers against the corrosion process by filling in crevices, gaps and micron holes in the composite coatings [16, 45-46, 48]. The MWCNTs were uniformly distributed in the alloy matrix and increased the corrosion potential of composite coatings toward more positive values, restricting localized corrosion, resulting in mainly homogenous corrosion. Furthermore, in both acidic and alkaline saline environments, Ni-W/MWCNTs composite coatings exhibit higher resistance to corrosion compared to Ni-W deposit coatings, and the behavior of these composite coatings shows the same tendency in 10 wt-% HCl solution. With increasing temperature, the composite coatings exhibit a better thermal stability compared to the Ni-W deposit coatings.

Acknowledgements

YH gratefully acknowledges Prof. H. Wang Analysis and Testing Center of Sichuan University for useful discussions and supports. The authors thank H. Wang for assistance with SEM and EDS measurements. The Applied Basic Research Project in Sichuan Province (2013JY0099) supported this work.

References

- [1] N. Eliaz, T. M. Sridhar, E. Gileadi, *Electrochim. Acta.* 2005, 50, 2893-2904.
- [2] M. P. Q. Argañaraz, S. B. Ribotta, M. E. Folquer, L. M. Gassa, G. Benítez, M. E. Vela, R. C. Salvarezza, *Electrochim. Acta.* 2011, 56, 5898-5903.
- [3] K. H. Hou, Y. F. Chang, S. M. Chang, C. H. Chang, *Thin. Solid. Films.* 2010, 518, 7535-7540.
- [4] H. Alimadadi, M. Ahmadi, M. Aliofkhazraei, S. R. Younesi, *Mater. des.* 2009, 30, 1356-1361.
- [5] F. Z. Yang, Y. F. Guo, L. Huang, S. K. Xu, S. M. Zhou, *Chinese. J. Chem.* 2004, 22, 228-231.
- [6] A. R. Jones, J. Hamann, A. C. Lund and C. A. Schuh, National Association for Surface Finishing Annual Technical Conference, 2009, (SUR/FIN 2009).
- [7] E. Beltowska-Lehman, P. Indyka, A. Bigos, M. Kot, L. Tarkowski, *Surf. Coat. Tech.* 2012, 211, 62-66.
- [8] I. Corni, R. J. Chater, A. R. Boccaccini, M. P. Ryan, *J. Mater. Sci.* 2012, 47, 5361-5373.
- [9] *Ceramics International*, 2013, 39, 2827-2834.
- [10] K. H. Hou, H. H. Sheu, M. D. Ger, *Appl. Surf. Sci.* 2014, 308, 372-379.
- [11] Y. W. Yao, S. W. Yao, L. Zhang, *Mater. Sci. Tech.* 2008, 24, 237-240.
- [12] Y. Boonyongmaneerat, K. Saengkiattiyut, S. Saenapitak, S. Sangsuk, *J. Alloys. Compd.* 2010, 506, 151-154.
- [13] B. Han, X. Lu, *Surf. Coat. Tech.* 2008, 202, 3251-3256.

- [14] R. A. C. Santana, A. R. N. Campos, E. A. Medeiros, A. L. M. Oliveira, L. M. F. Silva, S. Prasad, *J. Mater. Sci.* 2007, 42, 9137-9144.
- [15] R. A. C. Santana, S. Prasad, A. R. N. Campos, F. O. Araújo, G. P. da Silva, P. de Lima-Neto, *J. Appl. Electrochem.* 2006, 36, 105-113.
- [16] S. Khabazian, S. Sanjabi, *Appl. Surf. Sci.* 2011, 257, 5850-5856.
- [17] C. K. Lee, *Tribol. Int.* 2012, 55, 7-14.
- [18] C. R. Carpenter, P. H. Shipway, Y. Zhu, *Wear.* 2011, 271, 2100-2105.
- [19] I. Zambla, S. Varvara, L. M. Muresan, *J. Mater. Sci.* 2011, 46, 6484-6490.
- [20] M. S. Chandrasekar, M. Pushpavanam, *Electrochim. Acta.* 2008, 53, 3313-3322.
- [21] N. Imaz, E. Garcia-Lecna, J. ADiez, *Trans. Inst. Met. Finish.* 2010, 88, 256-261.
- [22] N.S. Qu, D. Zhu, K. C. Chan, W. N. Lei, *Surf. Coat. Tech.* 2003, 168, 123-128.
- [23] S. T. Song, D. DYL. Li, *Nanotech.* 2006, 17, 65-78.
- [24] Y. L. Yang, Y. D. Wang, Y. Ren, C. S. He, J. N. Deng, J. Nan, J. G. Chen, L. Zuo, *Mater. Lett.* 2008, 62, 47-50.
- [25] B. Praveen, T. Venkatesha, *J. Alloys Compd.* 2009, 482, 53-57.
- [26] C. Wang, M. Waje, X. Wang, J. M. Tang, R. C. Haddon, Y. Shan, *Nano Lett.* 2004, 4, 345-348.
- [27] S. Arai, A. Fujimori, M. Murai, M. Endo, *Mater. Lett.* 2008, 62, 3545-3548.
- [28] S. Khabazian, S. Sanjabi, *Appl. Surf. Sci.* 2011, 257, 5850-5856.
- [29] P. Martis, V.S. Dilimon, J. Delhalle, Z. Mekhalif, *Mater. Chem. Phys.* 2011, 128, 133-140.
- [30] C.R. Carpenter, P.H. Shipway, Y. Zhu, *Wear.* 2011, 271, 2100-2105.

- [31] R. Rastogi, R. Kaushal, S. K. Tripathi, A. L. Sharma, I. Kaur, L. M. Bharadwaj, *J. Colloid. Interface. Sci.* 2008, 328, 421-428.
- [32] A. Schierz, H. Zänker, *Environ. Pollut.* 2009,157, 1088-1094.
- [33] J. Zhang, H. Zou, Q. Qing, Y. Yang, Q. Li, Z. Liu, X. Guo, Z. Du, *J. Phys. Chem.* 2003, 107, 3712-3718.
- [34] S. Goyanes, G.R. Rubiolo, A. Salazar, A. Jimeno, M.A. Corcuera, I. Mondragon, *Diamond Relat. Mater.* 2007, 16, 412-417.
- [35] W. S. Lin, X. Y. Zhou, S. J. Wang, T. Li, *Material for Mechanical Engineering.* 2005, 4, 51-53.
- [36] Y. Suzuki, S. Arai, M. Endo, *J. Chem. Soc.* 2010, 157, D50-D53.
- [37] Lee, *Tribol. Int.* 2012, 55, 7-14.
- [38] Bercot. P, Peřna-Muřnoz. E, Pagetti. J. *Surf. Coat. Tech.* 2002, 157, 282.
- [39] X.H. Chen, C.S. Chen, H.N. Xiao, *Tribol. Int.* 2006, 39, 22.
- [40] M. Wang, Z. Wang, Z. Guo, *Mater. Chem. Phys.* 2014,148, 245-252.
- [41] O. Younes, L. Zhu, Y. Rosenberg, Y. Shacham-Diamand, E. Gileadi, *Langmuir.* 2001, 17, 8270-8275.
- [42] Z. Yang, H. Xu, Y.-L. Shi, M.-K. Li, Y. Huang, H.-L. Li, *Mater. Res. Bull.* 2005, 40, 1001.
- [43] J.N. Balaraju, V. EzhilSelvi, V.K. William Grips, K.S. Rajam, *Electrochim. Acta* 2006, 52, 1064–1074.
- [44] Z. Yang, H. Xu, M.K. Li, Y.L. Shi, Y. Huang, H.L. Li, *Thin Solid Films.* 2004, 466, 86-91.
- [45] X. H. Chen, C. S. Chen, H. N. Xiao, F. Q. Cheng, G. Zhang, G.J. Yi, *Surf. Coat. Technol.* 2005, 191, 351-56.
- [46] O. Younes, E. Gileadi, *J. Electrochem. Soc.* 2002,149,C100-C111.
- [47] M. Alishahi, S. M. Monirvaghefi, A. Saatchi, S. M. Hosseini, *Appl. Surf. Sci.* 2012, 258, 2439-2446.
- [48] S. Ranganatha, T. V. Venkatesha, K. Vathsala, *Ind. Eng. Chem. Res.* 2012, 51, 7932-7940.
- [49] S. Ranganatha, T. V. Venkatesha, K. Vathsala, *Appl. Surf. Sci.* 2012,263, 149-156.